

A Fluorescent Guanosine Dinucleoside as a Selective Switch-On Sensor for *c-myc* G-Quadruplex DNA with Potent Anticancer Activities

Y. Pavan Kumar,^[a] Sudipta Bhowmik,^[a] Rabindra Nath Das,^[b] Irene Bessi,^[c] Sushovan Paladhi,^[a] Rita Ghosh,^[d] Harald Schwalbe,^[c] and Jyotirmayee Dash*^[a, b]

Dedicated to Professor Krishna N. Ganesh on the occasion of his 60th birthday

Development of fluorescent chemical probes that can recognize biomacromolecules with high specificity and interfere with cellular processes is an emerging trend in chemical biology.^[1,2] Within this context, G-quadruplex DNA has received considerable attention as a prospective target for designing anticancer drugs.^[3-4] G-Quadruplex structures are widespread in the genome, found at the end of telomeres, in the promoter regions proto-oncogenes, and in the untranslated regions of mRNAs. These structures are believed to play key roles in the human genome, such as telomere maintenance and gene regulation.^[4] While several classes of molecules have been reported for stabilization of G-quadruplex DNA, only a few fluorescent chemosensors for the selective detection of G-quadruplex motifs have been developed.^[5,6] In addition, there is current interest in developing fluorescent probes with multiple signals that can find applications in analytical and computational devices.^[1-2,7] Recently we have shown that it is possible to create biomolecular logic-gate systems based on the interaction of fluorescent molecular probes with the G-quadruplex DNA.^[5f]

Monchaud and co-workers have reported the design and synthesis of two molecules containing guanine bases and their possible self-assembly to form artificial G-quartets as a nature-inspired strategy to interact with the G-quadruplex.^[8] These ligands show selectivity for quadruplexes over duplex

DNA. However, the G-quartets (self-assembled Hoogsteen-type hydrogen-bonded macrocycles of four guanine bases) are common to all quadruplexes, making discrimination between the quadruplexes challenging.

Previously we have reported synthesis of G-quadruplex binding ligand^[9] using “click-chemistry”^[9c] and fabrication of complex nanoarchitectures using supramolecular self-assembly of guanosine derivatives.^[10] Among the five natural nucleobases, guanosine and its derivatives have received considerable interest in supramolecular chemistry and nanotechnology.^[11] Taking inspiration from the natural self-organization of nucleosides, we envisioned designing a flexible ligand by linking a biocompatible fluorescent tag between two guanosine units using Cu^I-catalyzed 1,3-dipolar azide-alkyne cycloaddition.^[12,13] We hypothesized that the guanosine units can interact with the G-quartet of the quadruplex by means of hydrogen bonding and the flexible linker can tether in the groove region of quadruplex sequences. Since quadruplex sequences vary in the groove and loop regions, the ligand may show selectivity for a particular quadruplex sequence, for which the groove region would be maximally occupied. Further the ligand based on a guanosine nucleoside can be incorporated into DNA and the attached fluorophore would enable visualization of the nucleus in living cells.^[14]

Based on our design principle, we have synthesized a guanosine azide **1** from the natural nucleobase guanosine in three steps and a biocompatible fluorescent dansyl probe **2** (Scheme 1 and Scheme S1 in the Supporting Information). The C₂-symmetric dinucleoside **3** (DDG) was prepared in high yields by employing a double click reaction of **1** with the dansyl dialkyne **2** in the presence of Na ascorbate and CuSO₄·5H₂O in *t*BuOH/H₂O (1:1).

The ability of DDG to discriminate nucleic acid sequences was investigated using fluorescence spectroscopy (Figure 1). The emission spectra of the guanosine-dansyl conjugate DDG was characterized by a twofold intense peak at 430 nm and a minor peak at 553 nm, when excited at 350 nm (quantum yield, $\Phi=0.25$). Guanosine azide **1** is essentially non-fluorescent; however, the emission bands of DDG at 430 and 553 nm were assigned to the guanosine and the dansyl group, respectively, owing to the excitation energy transfer from the guanosine to the dansyl chromo-

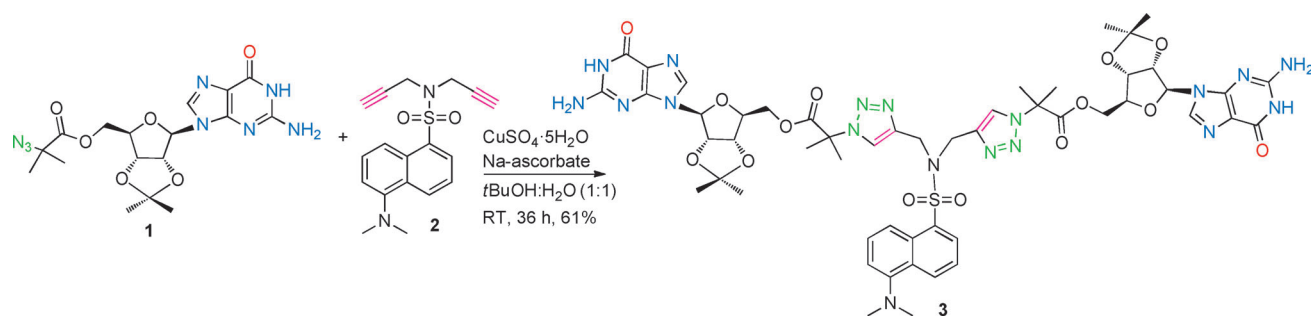
[a] Y. P. Kumar, Dr. S. Bhowmik, S. Paladhi, Prof. Dr. J. Dash
Department of Organic Chemistry
Indian Association for the Cultivation of Science Jadavpur
Kolkata-700032 (India)
E-mail: ocjd@iacs.res.in

[b] R. N. Das, Prof. Dr. J. Dash
Department of Chemical Sciences
Indian Institute of Science Education and Research Kolkata
Mohanpur, West Bengal 741252 (India)

[c] I. Bessi, Prof. Dr. H. Schwalbe
Institute of Organic Chemistry and Chemical Biology
Goethe University Frankfurt and
Center for Biomolecular Magnetic Resonance
Max-von-Laue Strasse 7, 60438 Frankfurt am Main (Germany)

[d] R. Ghosh
Department of Biochemistry and Biophysics
University of Kalyani, Kalyani-741235, West Bengal (India)

Supporting information for this article is available on the WWW under <http://dx.doi.org/10.1002/chem.201302107>.



Scheme 1. Modular synthesis of a fluorescent guanosine dinucleoside **3** (DDG).

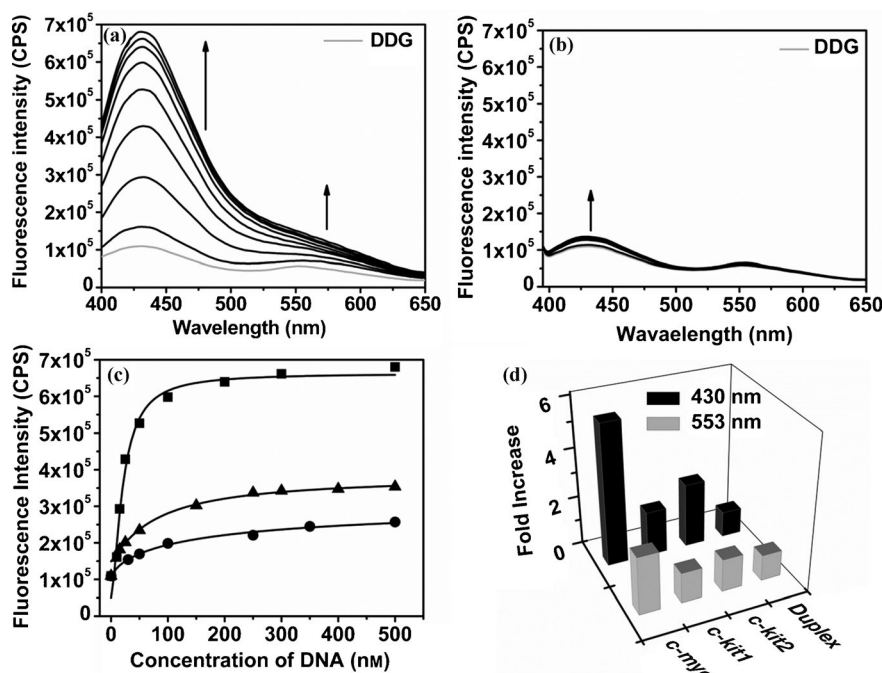


Figure 1. Fluorimetric titration spectra of DDG (500 nm) with a) *c-myc* quadruplex DNA (0–500 nm) and b) with duplex DNA (0–1500 nm). c) Fluorescence intensity profiles of DDG (500 nm) with quadruplex sequences (0–500 nm) at 430 nm (■ = *c-myc*, ● = *c-kit1*, ▲ = *c-kit2*). d) Fold increase of fluorescence intensity for DDG (500 nm) upon titration with DNA sequences (100 nm).

phore.^[15,16] This indicates that DDG, which contains biologically active non-natural and natural components, such as dansyl sulphonamide, triazole and guanosine, exhibits distinct optical properties and may lead to enhance biological activities.

When the fluorimetric titration of DDG (500 nm) was carried out at pH 7.4 with increasing concentration of quadruplex sequences (0–500 nm), the fluorescence intensity of both dansyl and guanosine band was enhanced in a dose-dependent manner from which the dissociation binding constants (K_d) were calculated (Figure 1 and Figures S2 and S3 and Table S1 in the Supporting Information).^[17] In the emission spectra, the addition of *c-myc* resulted higher selectivity, with a 6-fold enhancement of guanosine band and 2.5-fold enhancement for the dansyl band. It shows high selectivity for *c-myc* over *c-kit2* and *c-kit1* quadruplexes and

duplex DNA (Figure 1d). A negligible fluorescence enhancement of DDG was observed for duplex DNA at both the guanosine and dansyl bands. By comparing the change in ratio of the fold increase between guanosine and dansyl emission of DDG upon titration with DNA sequences, it was observed that in all cases the guanosine band was increased from one- to fourfold compared to the dansyl band. The ratiometric variation of DDG was dependent upon the nucleic acid sequences and recognition occurred at very low concentration of DNA. Interestingly, even in the presence of 100 nm *c-myc*, the emission intensity of DDG was increased fivefold at 430 nm (Figure 1d). It is important to point out that such nanomolar sensitivity is highly impressive for the development of biomarker for the quadruplex DNA. To the best

of our knowledge, none of the previously reported probes can detect nanomolar DNA with high selectivity.^[5] DDG showed both excellent affinity for *c-myc* quadruplex ($K_d = 20.8$ nm) as well as substantial specificity (44.5-fold) over duplex DNA ($K_d = 925.7$ nm) at 430 nm. DDG also exhibited 3.8-fold selectivity for *c-myc* over *c-kit2* ($K_d = 79.4$ nm) and 7.6-fold selectivity for *c-myc* over *c-kit1* ($K_d = 158.8$ nm).

Based on the high specificity of the guanosine–dansyl conjugate for *c-myc* quadruplex DNA, we performed excited-state lifetime measurements^[18] of DDG in the absence and presence of *c-myc* quadruplex DNA (Figure 2). The results reveal that DDG has two forms in the excited state, a major component (95.5%) with a lifetime of 454 ps and a minor form with a higher lifetime (1.7 ns). Upon addition of 1.0 equivalents of *c-myc* quadruplex, an enhancement in the excited state lifetime of both the species was observed.

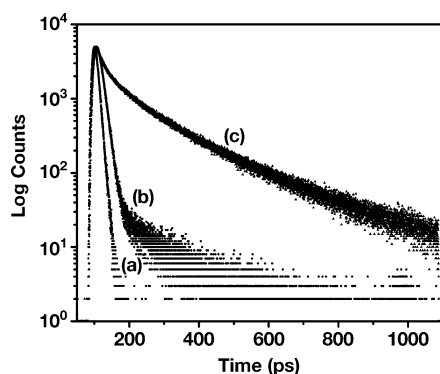


Figure 2. Fluorescence decay profiles ($\lambda_{\text{ex}} = 340$ nm) of a) the excitation lamp profile, b) DDG (500 nm), and c) DDG and *c-myc* (500 nm).

However, the decay profiles show that the minor form becomes the major component (75%) with a higher lifetime of 6.4 ns (Table S2, in the Supporting Information). These results indicate that DDG binds to *c-myc* G-quadruplex DNA and forms a stable complex with higher fluorescence as well as higher lifetime.

The interaction of DDG with G-quadruplex DNA was further evaluated by Förster resonance energy transfer (FRET) melting analysis^[19] using dual-labeled DNA sequences (Figure S4 in the Supporting Information). FRET melting analysis has been used to determine the G-quadruplex stabilization and selectivity of a ligand towards a particular G-quadruplex target. We have evaluated the melting of four DNA sequences with G-rich DNA sequences found in the promoter of *c-myc*, two G-quadruplexes found in the promoter of *c-kit* (*c-kit1* and *c-kit2*), and a self-complementary duplex DNA sequence. FRET melting studies showed good agreement with the fluorescence binding titrations (Table S3 in the Supporting Information). The stabilization potential for *c-myc* saturates at 1 μM concentration of DDG ($\Delta T_m = 12.6$ K at 1 μM , that is, a T_m of 93°C). DDG also showed good stabilization for *c-kit* quadruplex sequences with a ΔT_m of 17.5 K for *c-kit1* and ΔT_m of 7.4 K for *c-kit2* at a DDG concentration of 1 μM , whereas no detectable duplex stabilization ($\Delta T_m = 0.5^\circ\text{C}$) was observed for the DDG at this concentration.

To shed light on the binding mode, the titration of DDG with *c-myc* DNA was monitored by 1D ^1H NMR spectra (Figure 3). In the region of imino proton signals, NMR resonances from G13, G14/G4 (overlapped signals) residues revealed significant line broadening. Also in the aromatic region, changes in chemical shifts could not be quantified for all residues due to signal overlap. Among the monitored aromatic protons, residues G2, A12, G13, and A22 showed the most pronounced chemical-shift perturbations. Further, in the ^1H , ^1H -NOESY spectrum (Figure 3c), the cross-peak of imino signal of G6 to G5 and of G6* to G5* in the second minor conformation of *c-myc*^[20] is shifted, suggesting that G6 is interacting with the ligand. Furthermore, the cross-peaks of imino signal of G13 to G8, G9 and G14 are much weaker in the presence of the ligand than in the free

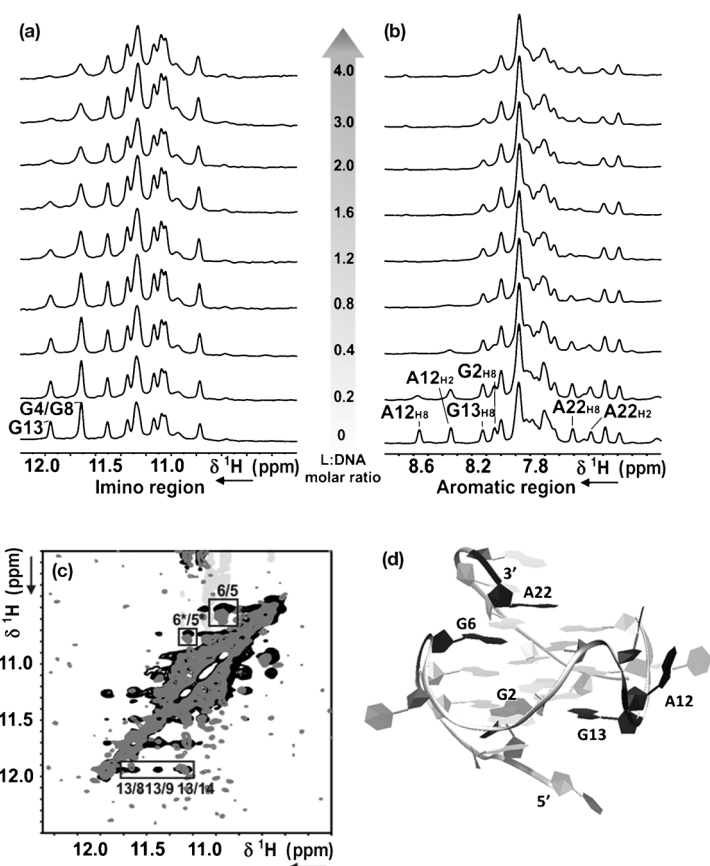


Figure 3. NMR spectra (600 MHz) of a) the imino region and b) the aromatic region of 200 μM *c-myc* in the presence of DDG at different DDG:*c-myc* DNA molar ratio. c) Overlay of imino region of ^1H , ^1H -NOESY of the complex (grey: *c-myc*:DDG=1:2, 300 μM *c-myc*, 800 MHz) with the DNA alone (black: 1 mM *c-myc*, 950 MHz); Titration was performed at 298 K, in buffer containing 25 mM tris-HCl at pH 7.4 and 100 mM KCl, $\text{H}_2\text{O}/[\text{D}_6]\text{DMSO}$ 80:20. d) Map of chemical shift perturbations detected by NMR spectroscopy on the *c-myc* model (PDB: 1XAV); adenosine and guanine perturbed residues in black.

from, confirming that G13 must be involved in the interaction with DDG, in line with the NMR data from titration experiments. Our initial NMR analysis therefore shows that DDG interacts with both the external G-quartets and with the groove defined by G8-G9-G10 and G13-G14-G15 (Figure 3d).

Human malignant melanoma A375 cells were used as a model to investigate the cell membrane permeability of DDG (Figure 4). The cells were incubated with DDG (2.5 μM) for 30 min at 37°C and examined by fluorescence microscopy. It was found that DDG, which contains the guanosine nucleoside unit and hydrophobic heteroaromatic core, is cell-membrane permeable and displays blue fluorescence (Figure 4b). The images indicated that DDG binds to the nucleus preferentially, but it also stains other parts of the cell. This result was further confirmed by co-staining DDG with the nucleus marker propidium iodide (PI; Figure 4c).

The antiproliferative activities of the dansyl-guanosine conjugate DDG was then determined on the A375 cell line.

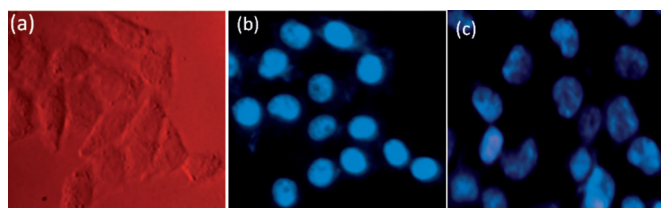


Figure 4. Fluorescence microscope images of A375 cells. a) Bright-field transmission image of cells after incubation with DDG (2.5 μM) at 37°C for 30 min. b) Fluorescence image of a). c) Fluorescence image of DDG stained (same as a) fixed with 4% paraformaldehyde and stained with PI (1.0 μM) for 30 min.

The cytotoxic effect of DDG on A375 cells was determined with varying concentrations (0, 0.5, 1, 10, 25, 50 μM) for 24 h by MTT assay (MTT = 3-(4,5-dimethylthiazol-2-yl)-2,5-diphenyltetrazolium bromide).^[21] The IC_{50} value of DDG was found to be 5 μM (Figure S5 in the Supporting Information). Despite this potency, DDG exhibited lower cytotoxicity towards human normal keratinocyte (HaCaT) cells with an IC_{50} value at 69 μM . These results suggest that DDG possess significant selectivity for cancer cells over normal cells. Next we have investigated the ability of DDG to arrest the cell cycle and induce apoptosis using A375 cells by fluorescence-activated cell sorting (FACS).^[22–24] The cell cycle analysis revealed that DDG can disturb the cell cycle of the A375 cell line after exposure for only 12 h, which is shown with the decreased G0–G1 phase and an increased G2/M phase in a dose-dependent manner (Figure S6 in the Supporting Information). The treatment of DDG caused cell cycle arrest in G2/M phase,^[25] possibly due to repair of damaged DNA phase.

To determine whether the observed cell death induced by DDG was due to apoptosis, a biochemical marker of apoptosis, for example, mitochondrial membrane depolarization (Ψ_m), was monitored by flow cytometry after JC-1 staining.^[22–24] As shown in Figure 5, untreated cells have intact mitochondria and normal $\Delta\Psi_m$; however, the loss of $\Delta\Psi_m$ exhibits a dose-dependent increase after the cells were treated with DDG, as evidenced by the shift of fluorescence of the JC-1 dye from red to green. DDG at the concentrations of 1, 2.5 and 5 μM for 24 h increased $\Delta\Psi_m$ of cells from 8.36 to 39.06, 46.27, and 50.27%, respectively. These experiments indicated that cancer cells treated by DDG lose $\Delta\Psi_m$ and induce apoptosis in A375 cells through mitochondria-mediated pathways. The viability of A375 cells treated with DDG was further investigated by PI-flow cytometric analysis.^[24] The in vitro apoptosis analysis indicated that exposure of A375 cells to different concentrations of DDG for 24 h resulted in a dose-dependent increase in the proportion of apoptotic cells (16.06 to 36.11%, Figure S7 in the Supporting Information).

We have shown here the first example of a synthetic guanosine-based novel fluorescent biosensor that shows rapid, selective, and sensitive turn-on responses to nucleic acid sequences. The fluorescence enhancement of the dansyl guanosine derivative in the presence of *c-myc* DNA occurs in

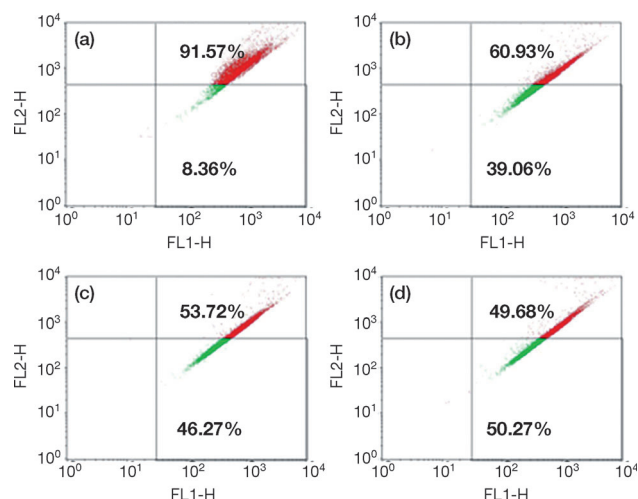


Figure 5. Flow cytometric analysis of the change in mitochondrial potential. A375 cancer cells were incubated for 24 h in the presence of (0–5 μM) of DDG using JC1-stained cells. Histograms a) 0 μM , b) 1.0 μM , c) 2.5 μM , and d) 5.0 μM indicate the percent of normal (M1) and apoptotic cells (M2) upon treatment with DDG.

real time, which could potentially be developed as a biomarker for the quadruplex in the nanomolar concentration range. Dinucleoside DDG induces cell cycle arrest at G2/M phase, exhibits specific cytotoxicity to the human melanoma A375 cells over normal human keratinocyte cells, and promotes cell death by apoptosis.

Acknowledgements

This work was supported by the Department of Science and Technology (DST), Department of Biotechnology (DBT) and Council of Science and Industrial Research (CSIR), India. R.N.D. and S.P. thank CSIR India for research fellowships. The authors thank Prof. Dr. Shankar Balasubramanian, University of Cambridge, and Prof. Dr. Kankan Bhattacharyya, IACS Kolkata, for helpful comments on the manuscript.

Keywords: cell cycles • click chemistry • fluorescence • nucleosides • G-quadruplex DNA

- [1] a) A. W. Czarnik, *Fluorescent Chemosensors for Ion and Molecule Recognition*, American Chemical Society, Washington, DC, **1992**; b) A. P. de Silva, in *Molecular and Supramolecular Chemistry. Vol. 7: Supramolecular Devices* (Eds.: J. W. Steed, P. A. Gale, P. Anzenbacher), Wiley-Blackwell, Oxford, **2012**, p. 2497.
- [2] a) A. P. de Silva, S. Uchiyama, *Nat. Nanotechnol.* **2007**, *2*, 399–410; b) M. S. T. Gonçalves, *Chem. Rev.* **2009**, *109*, 190–212; c) R. W. Sinkeldam, N. J. Greco, Y. Tor, *Chem. Rev.* **2010**, *110*, 2579–2619; d) R. N. Dsouza, U. Pischel, W. M. Nau, *Chem. Rev.* **2011**, *111*, 7941–7980; e) X. Chen, X. Tian, I. Shin, J. Yoon, *Chem. Soc. Rev.* **2011**, *40*, 4783–4804; f) X. Chen, T. Pradhan, F. Wang, J. S. Kim, J. Yoon, *Chem. Rev.* **2012**, *112*, 1910–1956; g) M. Vendrell, D. Zhai, J. Cheng, Y. T. Chang, *Chem. Rev.* **2012**, *112*, 4391–4420.
- [3] S. Neidle, S. Balasubramanian, *Quadruplex Nucleic Acids*, Royal Society of Chemistry, Cambridge (UK), **2006**.
- [4] a) J. T. Davis, *Angew. Chem.* **2004**, *116*, 684–716; *Angew. Chem. Int. Ed.* **2004**, *43*, 668–698; b) D. Monchaud, M. P. Teulade-Fichou, *Org.*

- Biomol. Chem.* **2008**, *6*, 627–636; c) Y. Qin, L. H. Hurley, *Biochimie* **2008**, *90*, 1149–1171; d) S. Balasubramanian, S. Neidle, *Curr. Opin. Chem. Biol.* **2009**, *13*, 345–353; e) S. Balasubramanian, L. H. Hurley, S. Neidle, *Nat. Rev. Drug Discovery* **2011**, *10*, 261–275; f) G. W. Collie, G. N. Parkinson, *Chem. Soc. Rev.* **2011**, *40*, 5867–5892; g) M. L. Bochman, K. Paeschke, V. A. Zakian, *Nat. Rev. Genet.* **2012**, *13*, 770–780.
- [5] For a review, see: a) E. Largy, A. Granzhan, F. Hamon, D. Verga, M.-P. Teulade-Fichou, *Top. Curr. Chem.* **2012**, *330*, 111–178. For selected examples, see: b) F. Koeppl, J. F. Riou, A. Laoui, P. Mailliet, P. B. Arimondo, D. Labit, O. Petitgenet, C. Helene, J. L. Mergny, *Nucleic Acids Res.* **2001**, *29*, 1087–1096; c) P. Yang, A. De Cian, M. P. Teulade-Fichou, J. L. Mergny, D. Monchaud, *Angew. Chem.* **2009**, *121*, 2222–2225; *Angew. Chem. Int. Ed.* **2009**, *48*, 2188–2191; d) M. Nikan, M. Di Antonio, K. Abecassis, K. McLuckie, S. Balasubramanian, *Angew. Chem. Int. Ed.* **2013**, *52*, 1428–1431; e) J. Mohanty, N. Barooah, V. Dhamodharan, S. Hari Krishna, P. I. Pradeepkumar, A. C. Bhasikuttan, *J. Am. Chem. Soc.* **2013**, *135*, 367–376; f) S. Bhowmik, R. N. Das, B. Parasar, J. Dash, *Chem. Commun.* **2013**, *49*, 1817–1819; and references there in.
- [6] For selected metal complexes, see: a) K. Suntharalingam, Łęczkowska, M. A. Furrer, Y. Wu, M. K. Kuimova, B. Therrien, A. J. P. White, R. Vilar, *Chem. Eur. J.* **2012**, *18*, 16277–16282; b) J. Alzeer, B. R. Vummidi, P. J. C. Roth, N. W. Luedtke, *Angew. Chem.* **2009**, *121*, 9526–9529; *Angew. Chem. Int. Ed.* **2009**, *48*, 9362–9365; and references there in.
- [7] H.-Z. He, D. S.-H. Chan, C.-H. Leung, D.-L. Ma, *Nucleic Acids Res.* **2013**, *41*, 4345–4359.
- [8] a) L. Stefan, A. Guédin, S. Amrane, N. Smith, F. Denat, J. L. Mergny, D. Monchaud, *Chem. Commun.* **2011**, *47*, 4992–4994; b) H. J. Xu, L. Stefan, R. Haudecoeur, S. Vuong, P. Richard, F. Denat, J. M. Barbe, C. P. Gros, D. Monchaud, *Org. Biomol. Chem.* **2012**, *10*, 5212–5218; c) R. Haudecoeur, L. Stefan, F. Denat, D. Monchaud, *J. Am. Chem. Soc.* **2013**, *135*, 550–553.
- [9] a) J. Dash, P. S. Shirude, S. Balasubramanian, *Chem. Commun.* **2008**, 3055–3057; b) J. Dash, P. S. Shirude, S. T. D. Hsu, S. Balasubramanian, *J. Am. Chem. Soc.* **2008**, *130*, 15950–15956; c) J. Dash, Z. A. E. Waller, G. D. Pantoş, S. Balasubramanian, *Chem. Eur. J.* **2011**, *17*, 4571–4581; d) J. Dash, R. N. Das, N. Hegde, G. D. Pantoş, P. S. Shirude, S. Balasubramanian, *Chem. Eur. J.* **2012**, *18*, 554–564.
- [10] a) J. Dash, A. J. Patil, R. N. Das, F. Dowdal, S. Mann, *Soft Matter* **2011**, *7*, 8120–8126; b) R. N. Das, Y. P. Kumar, S. Pagoti, A. J. Patil, J. Dash, *Chem. Eur. J.* **2012**, *18*, 6008–6014.
- [11] a) J. T. Davis, G. P. Spada, *Chem. Soc. Rev.* **2007**, *36*, 296–313; b) S. Lena, S. Masiero, S. Pieraccini, G. P. Spada, *Chem. Eur. J.* **2009**, *15*, 7792–7806.
- [12] V. V. Rostovtsev, L. G. Green, V. V. Fokin, K. B. Sharpless, *Angew. Chem.* **2002**, *114*, 2708–2711; *Angew. Chem. Int. Ed.* **2002**, *41*, 2596–2599.
- [13] a) F. Amblard, J. H. Cho, R. F. Schinazi, *Chem. Rev.* **2009**, *109*, 4207–4220; b) H. C. Kolb, K. B. Sharpless, *Drug Discovery Today* **2003**, *8*, 1128–1137.
- [14] Y. N. Teo, E. T. Kool, *Chem. Rev.* **2012**, *112*, 4221–4245.
- [15] J. R. Lakowicz, *Principles of Fluorescence Spectroscopy*, 2nd ed., Kluwer Academic/Plenum, New York, **1999**.
- [16] For PET based RNA sensors, see; B. A. Sparano, K. Koide, *J. Am. Chem. Soc.* **2007**, *129*, 4785–4794.
- [17] H. M. Kim, M. S. Seo, M. J. An, J. H. Hong, Y. S. Tian, J. H. Choi, O. Kwon, K. J. Lee, B. R. Cho, *Angew. Chem.* **2008**, *120*, 5245–5248; *Angew. Chem. Int. Ed.* **2008**, *47*, 5167–5170.
- [18] M. Y. Berezin, S. Achilefu, *Chem. Rev.* **2010**, *110*, 2641–2684.
- [19] a) R. A. J. Darby, M. Sollogoub, C. McKeen, L. Brown, A. Risitano, N. Brown, C. Barton, T. Brown, K. R. Fox, *Nucleic Acids Res.* **2002**, *30*, 39e; b) A. De Cian, L. Guittat, M. Kaiser, B. Sacca, S. Amrane, A. Bourdoncle, P. Alberti, M.-P. Teulade-Fichou, L. Lacroix, J. L. Mergny, *Methods* **2007**, *42*, 183–195.
- [20] a) A. Ambrus, D. Chen, J. Dai, R. A. Jones, D. Yang, *Biochemistry* **2005**, *44*, 2048–2058; b) J. Dai, M. Carver, L. H. Hurley, D. Yang, *J. Am. Chem. Soc.* **2011**, *133*, 17673–17680.
- [21] T. Mosmann, *J. Immunol. Methods* **1983**, *65*, 55–63.
- [22] C. Riccardi, I. Nicoletti, *Nat. Protoc.* **2006**, *1*, 1458–1461.
- [23] T. Liu, B. Hannafon, L. Gill, W. Kelly, D. Benbrook, *Mol. Cancer Ther.* **2007**, *6*, 1814–1822.
- [24] M. van Gurp, N. Festjens, G. van Loo, X. Saelens, P. Vandenabeele, *Biochem. Biophys. Res. Commun.* **2003**, *304*, 487–497.
- [25] For a G-quadruplex stabilizer that induces M-phase cell cycle arrest; see: Y.-C. Tsai, H. Qi, C.-P. Lin, R.-K. Lin, J. E. Kerrigan, S. G. Rzuczek, E. J. Lavoie, J. E. Rice, D. S. Pilch, Y. L. Lyu, L. F. Liu, *J. Biol. Chem.* **2009**, *284*, 22535–22543.

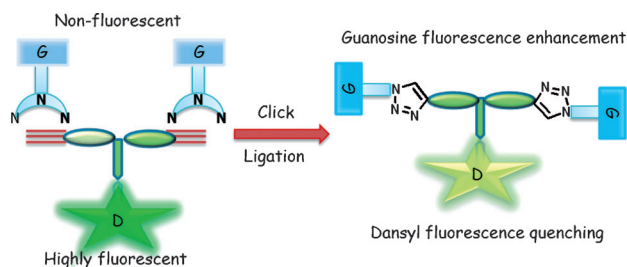
Received: June 3, 2013

Published online: ■ ■ ■, 0000

G-Quadruplex Detection

Y. P. Kumar, S. Bhowmik, R. N. Das,
I. Bessi, S. Paladhi, R. Ghosh,
H. Schwalbe, J. Dash* ■■■■-■■■■

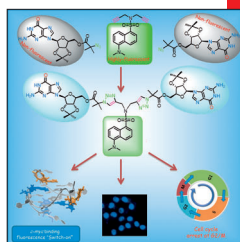
A Fluorescent Guanosine Dinucleoside as a Selective Switch-On Sensor for *c-myc* G-Quadruplex DNA with Potent Anticancer Activities



Like likes like! A novel fluorescent C_2 -symmetric guanosine-based dinucleoside has been engineered by chemical ligation of two guanosine units with a biocompatible dansyl tag that exhibits high selectivity for *c-myc* G-quadruplex DNA through fluorescence

enhancement over duplex DNA and other promoter G-quadruplexes (see scheme). It stains the nucleus preferentially, arrests the cell cycle at the G2/M phase, inhibits cell growth, and induces apoptosis in A375 cancer cells.

CHEMISTRY
A EUROPEAN JOURNAL
19/00 2013



WILEY-VCH

www.chemistry-journal.org

A fluorogenic guanosine-dansyl conjugate (depicted).....that detects G-quadruplex DNA through fluorescence enhancement has been developed by J. Dash et al. and reported in their Communication on page ■■ ff. This dinucleoside interacts with both the external G-quartets and in the groove regions of *c-myc* G-quadruplex DNA. It stains the nucleus preferentially and exhibit potent antiproliferative activities against A375 human melanoma cell line.